Journal of the Optical Society of Korea, Vol. 7, No. 2, June 2003, pp. 89-96

Control of Free Spectral Range of Long Period Fiber Grating by Cladding Mode Waveguide Dispersion

H. Jeong† and K. Oh*

Department of Information and Communications, Kwangju Institute of Science and Technology, Gwangju 500-712, KOREA

(Received April 8, 2003)

A new method to control the free spectral range of a long period fiber grating is proposed and theoretically analyzed. As the refractive index decreases radially outward in the silica cladding due to graded doping of fluorine, waveguide dispersion in the cladding modes was modified to result in the effective indices change and subsequently the phase matching conditions for coupling with the core mode in a long period fiber grating. Enlargement of the free spectral range in a long period fiber grating was theoretically confirmed.

OCIS codes : 050.2770, 060.2340, 230.0230.

I. INTRODUCTION

Long period gratings (LPGs) have been intensively studied for applications in optical communications and sensor systems due to benefits such as all-fiber configuration, low insertion loss, high flexibility in spectral design, and low cost. LPG devices have been developed in recent years as gain equalizers in erbium-doped fiber amplifiers (EDFA) for wavelength-division multiplexing (WDM) systems [1], bandpass filters, polarizers [2], demodulators [3] and sensing elements. In an LPG, a periodic index structure with a pitch of hundreds of microns imposes the phase-matching condition between the fundamental core mode and forward propagating cladding modes in an optical fiber, shown below,

$$\frac{2\pi n_{eff}^{11}(\lambda)}{\lambda} - \frac{2\pi n_{eff}^{lm}(\lambda)}{\lambda} = \frac{2\pi}{\Lambda} \qquad (1)$$

Here Λ is the grating pitch. And n_{eff}^{11} and n_{eff}^{lm} are the effective index of the HE_{11} core mode and that of the HE_{lm} cladding modes, respectively. Recently the gain bandwidth of optical amplifiers is rapidly expanding to fully exploit the bandwidth allowed in silica optical fibers. Examples are thulium-doped fiber amplifier (TDFA) for the S^+-band (1450−1490 nm) [4], fiber Raman amplifier (FRA) for the S-band (1490−1530 nm) [5], as well as combination of the conventional EDFA for the C-band (1530−1570 nm) [6] and the L-band (1570−1610 nm). [7] In spite of continuous development of ultra wide band amplifiers, an LPG optimized for a certain gain equalization filter could induce a high insertion loss in the neighboring gain bands because of the relatively close-spaced resonance peaks of the cladding modes. Fig. 1 shows this circumstance: Fig. 1 (a) shows a typical LPG's transmission spectrum used as a gain equalization filter in C-band EDFA and Fig. 1 (b) shows the same LPG's transmission spectrum in a wider wavelength range. Note that the gain equalization filter optimized for the C-band incurs additional insertion loss over 10 dB in 1.4 μm and 5 dB in 1.3 μm due to the closely spaced resonance cladding modes. The ability to control the free spectral range of the resonance peaks in LPGs, thus, is needed for novel fiber filters in ultra wide band optical communication systems.

There was a report about etching the fiber cladding with a HF acid solution to tune continuously the resonance wavelengths of long-period gratings. The method is based on the dependence of the propagation constants of the cladding modes on the cladding diameter. [8] And large resonance peak spacing based on the cladding-etched fiber was demonstrated by Li *et al.* in an acoustooptic tunable filter (AOTF). [9] However, the etched fiber shows very weak and poor long-term stability due to easy degradation by OH. [10] Also there is a problem of mass production.

In this paper we propose a new method to control the LPG spectrum by introducing waveguide dispersion into cladding modes. In previous studies in LPGs, direct modification of cladding mode waveguide dis-

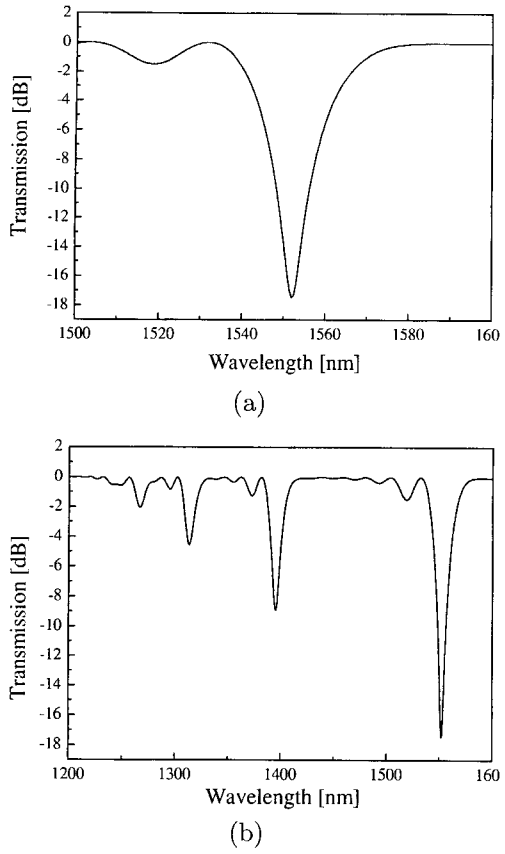

FIG. 1. Transmission spectrum for a typical long-period fiber grating for a C-band EDFA gain equalization filter in (a) 1500 nm−1600 nm wavelength range, (b) 1200 nm−1600 nm wavelength range.

persion and its subsequent effects on the spectra of LPGs have not been fully investigated so far. Recently the material dispersion change of cladding modes by doping transition metals and its impact on the free spectral ranges in LPG have been reported by the authors. [11] By a proper design of the refractive index profile, the magnitude of change in the effective indices of the cladding modes in the proposed fiber could be made large enough to affect the phase matching conditions for the coupling with the fundamental core mode. The phase matching conditions will subsequently affect LPG transmission spectra and the free spectral range. In this study the authors theoretically analyzed the effect of the refractive index profile of the cladding region on the LPG spectrum and proposed a new technique to enhance the free spectral range of LPG, for the first time to the best knowledge of the authors.

II. NUMERICAL ANALYSIS

The dispersive characteristics of binary silica glass doped with dopants such as GeO_2 and F have been precisely calculated using the Sellmeier equation for given ranges of concentrations. [12] The sellmeier equation for the refractive index n is given as below;

$$n^2 - 1 = \sum_{i=1}^{3} \frac{a_i \lambda^2}{\lambda^2 - b_i} \tag{2}$$

Sellmeier coefficients, denoted by ai and bi, for binary silica doped with GeO_2 and F are summarized in Table 1.

In fiber devices such as LPG and fiber acousto-optic filter, the main mechanism to generate a spectral response is the coupling between the fundamental mode (HE_{11}) guided through the core and the cladding modes guided through an air-silica multimode waveguide. In the analysis the core was assumed to be germanosilicate glass as in conventional single mode fibers (SMF). The refractive index of cladding was assumed to be depressed by gradual doping of fluorine (F) into silica glass to construct triangular and trapezoidal refractive index profiles. The authors strongly believe that fibers with a triangular or trapezoidal cladding waveguide could be fabricated by the OVD (Outside Vapor Deposition) method in which the refractive index profile of the cladding region can be easily controlled. [13] Especially, a LPG with a trapezoidal cladding waveguide is insensitive to the environmental change of the outside of cladding region, which induces major problems during packaging of a conventional LPG. The refractive index of air was set to 1.0 independent of wavelength. The mode field

TABLE 1. Sellmeier coefficients of binary silica glass doped with GeO_2 or F[12]. The coefficients are valid for spectral range of 0.4−1.7 μm.

mol%			Sellmeier coefficients					
SiO_2	GeO_2	F	a_1	b_1	a_2	b_2	a_3	b_3
100			0.6961663	0.004679148	0.4079426	0.01351206	0.8974994	97.934002
98.1	1.9		0.697505	0.004187707	0.413531	0.01454822	0.890266	98.219695
95.9	4.1		0.700071	0.004596176	0.421598	0.01448869	0.888017	98.203859
92.9	7.1		0.702680	0.005390188	0.429438	0.01453037	0.903376	119.67966
96.9		3.1	0.69325	0.004521218	0.39720	0.01372178	0.86008	95.572131
93.9		6.1	0.67744	0.003763823	0.40101	0.01447209	0.87193	97.146650

profiles of core and cladding modes could be calculated by finite-difference analysis with the inverse power iteration method. [14] With these assumptions, we could calculate the mode field profiles and intensity distributions of both the core and the cladding modes defined by the proposed fiber structure. The coupling coefficients between them could be calculated by the overlap integral for a given index perturbation.

If we limit the calculation to gratings that consist of perfect circular-symmetric index perturbation in the transverse plane of the fiber, the only nonzero coupling coefficients between the core mode and the cladding modes involve cladding modes of azimuthal number $l = 1$. [15] We will confine the calculation to only $l = 1$ cladding modes.

The coupled mode equation that describes interactions in an LPG is given by [15]

$$\frac{dA^{co}}{dz} = j\kappa(z)A^{co} + j\sum_m \frac{p}{2}\kappa(z)A_m^{cl}\exp(-j2\delta^{cl-co}z), \quad (3)$$

$$\frac{dA_m^{cl}}{dz} = j\sum_m \frac{p}{2}\kappa(z)A_m^{co}\exp(+j2\delta^{cl-co}z). \quad (4)$$

Here p stands for the induced-index fringe modulation, where $0 \le p \le 1$. And the coupling constant for core mode and cladding modes, $\kappa(z)$, and the phase shift, δ^{cl-co}, can be expressed as

$$\kappa(z) = \frac{\omega\epsilon_o n_1^2\sigma(z)}{} \times 2\int_0^{2\pi} d\phi \int_0^{a_1} r \times dr(E_r^{cl}E_r^{co^*} + E_\phi^{cl}E_\phi^{co^*}), \quad (5)$$

$$\delta^{cl-co} = \frac{1}{2}(\beta_{01}^{co} - \beta_{1m}^{cl} - \frac{2\pi}{\Lambda}). \quad (6)$$

Here $\sigma(z)$ is the normalized induced-index change in the core. A^{co} and A_m^{cl} are the amplitudes of the core mode and m-th cladding modes, respectively. Here we assumed that the induced-index change was uniform across the core such that $\sigma(z)$ was taken out of the overlap integral. By the boundary conditions that are $A^{co}(z = L/2) = 1$, and $A_m^{cl}(z = -L/2) = 0$, where L is the grating length, the transmission through the grating is simply given by $A^{co}(z = L/2)/A^{co}(z = -L/2)$. For propagation parameters $u_i^2 = k^2n_i^2 - \beta^2 = -w_i^2$, the electric fields of core and cladding modes for each boundary could be obtained by numerically solving Maxwell's equation as in. [16]

III. CLADDING MODE ANALYSIS

The effective indices of the first ten cladding modes were calculated for step, triangular and trapezoidal refractive index profiles. The waveguide dispersion as well as material dispersion calculated using the Sellmeier equation was taken into account in the numerical analysis. In this study, we modify the refractive index profile of the cladding region from the step waveguide to a triangular or a trapezoidal waveguide, as shown in Fig. 2, in order to change waveguide dispersion of cladding modes. Note that the core parameters were set similar to those of conventional SMF. In triangular profiles, Fig. 2(a), the refractive indices in the cladding linearly decrease to the minimum values, 1.454, 1.451, 1.448. The profiles are designated by the index difference relative to the pure silica clad in conventional step SMF. The refractive index difference was set by the experimental results where a conventional chemical vapor deposition process can work achieve with Fluorine containing precursors such as SiF_4, C_3F_8. [17] In trapezoidal profiles, the refractive index decreases linearly after a certain radial position, the upper pedestal of the trapezoid, in the cladding

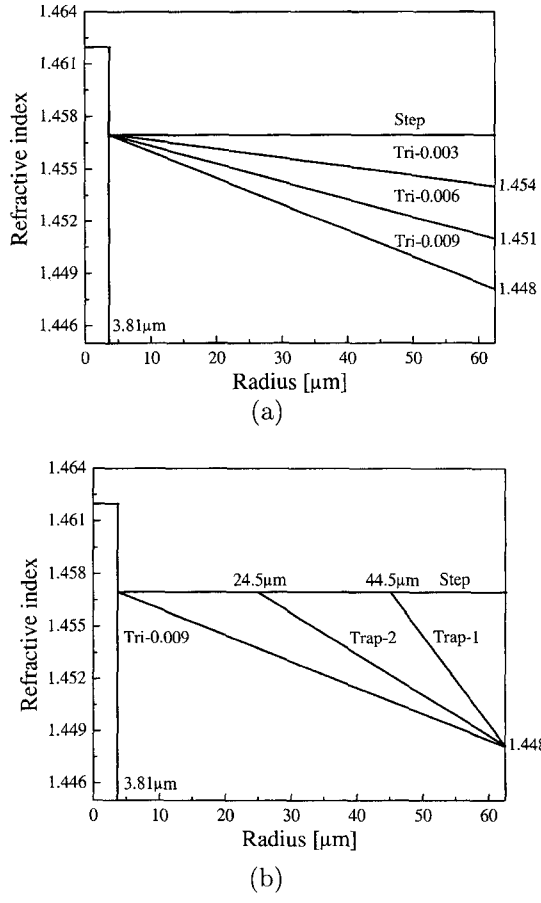

FIG. 2. Refractive index profile of the proposed fiber for triangular structure, (a), and trapezoidal structure, (b), evaluated at 0.6328 μm. Note that 0.003, 0.006 and 0.009 in (a) indicated the maximum clad-refractive index difference referenced to the step index profile. The minimum refractive index in the trapezoidal profiles was set to 1.448 with the index difference of 0.009.

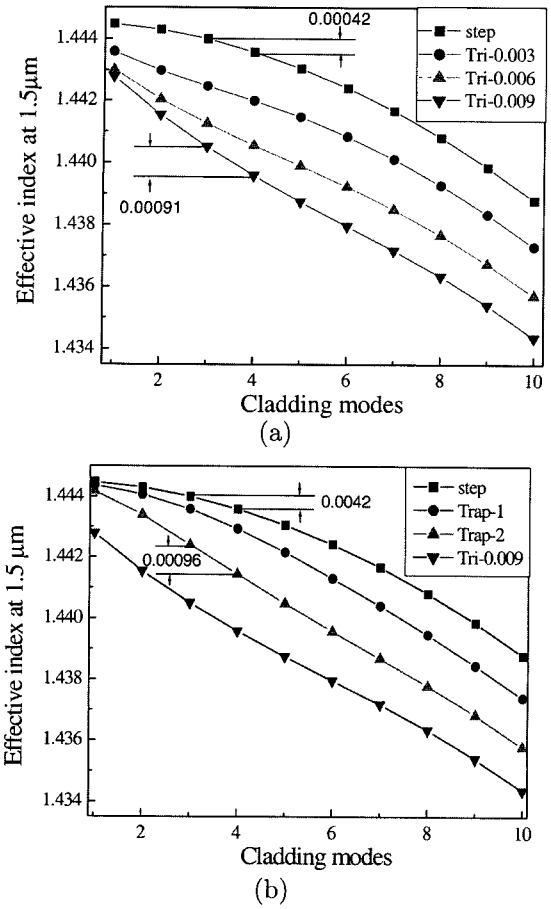

FIG. 3. Effective indices of cladding modes for (a) triangular refractive index profile, as shown in Fig. 2 (a), and (b) trapezoidal refractive index profile, as shown in Fig. 2 (b). Both material dispersion and waveguide dispersion are included in calculations.

the minimum index was set as 1.448, with the index difference of 0.009 relative to the pure silica clad.

By solving the characteristic equations for the guided modes [14–16] for different index profiles in Fig. 2, effective indices of the first ten cladding modes were numerically evaluated at 1.5 μm, and the calculated results are plotted in Fig. 3. Two significant modifications were observed. Firstly, the effective indices of the cladding modes decrease as much as by $\sim 1.7\times10^{-3}$ or by a factor of $\sim$0.12 % referenced to conventional step SMF, for the 0.009 triangular waveguide at the cladding mode number of 1 as in Fig. 3(a). And the difference in effective indices referenced to the step SMF gradually increases for higher order cladding modes. Similar effects were also observed in the trapezoidal waveguides as shown in Fig. 3(b). Induced change in effective refractive index for both structures is significant enough to change the phase matching conditions with the core mode. Secondly, the spacing in the effective indices between the adjacent modes does increases, which will directly affect the free spectral range. For example the effective index spacing between the third and fourth modes increases by a factor over 2, for the 0.009-triangular profile and Trapezoidal profile-2. These modifications are attributed to the effects of waveguide dispersion as well as the material dispersion due to fluorine doping. It is, therefore, expected from those observations that the waveguide modification in the cladding indeed modifies the phase matching conditions and subsequently the free-spectral range can be controlled. Detailed analysis of the phase matching and spectral response will be discussed in the following section.

The other important aspect in LPG spectrum analysis is the overlap integral between the core mode and the cladding mode, which will determine the strength of the resonant coupling as shown in Eq. (5). After finding mode fields of the fundamental core mode and the first ten cladding modes, the overlap integrals were evaluated at 1.5 μm. The results are presented for various index profiles in Fig. 4. In conventional step index SMF the overlap integral, or equivalently the coupling constant κ, increases in higher order cladding

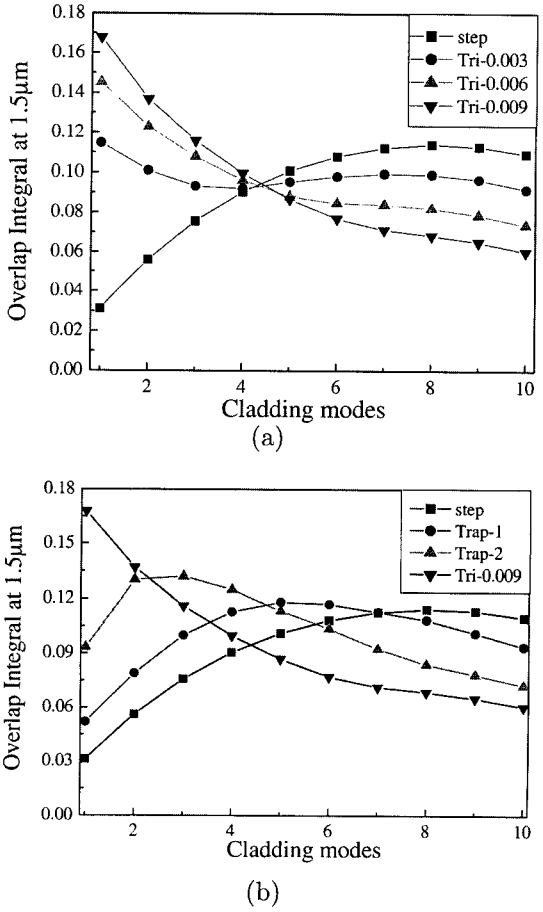

FIG. 4. Overlap integral between the fundamental core mode and cladding modes for triangular refractive index profile, (a), and trapezoidal refractive index profile, (b). The overlap integrals were evaluated at 1.5 μm.

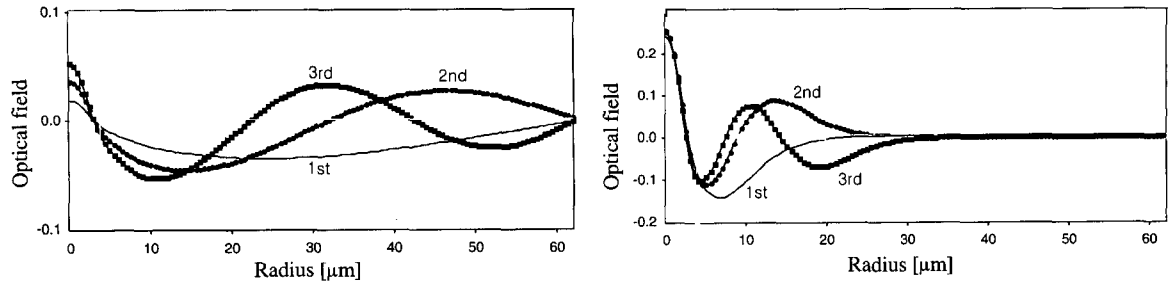

FIG. 5. Plots of the optical field as radial position for the first three cladding modes in a fiber having step index profile, (a), and having 0.009-triangular index profile, (b).

modes and reaches the maximum around the 8th mode, as reported in reference. [15] In the case of the triangular and the trapezoidal waveguides, however, the overlap integral shows contrasting characteristics. Especially, in the triangular waveguide the overlap integral has its maximum at the 1st cladding mode and decreases in higher order modes. Similarly in trapezoidal profiles, the overlap integral reaches its maximum in a lower order mode than for step index SMF. To explain this feature, mode field distribution was calculated for step and triangular index profile. Fig. 5 shows the calculated mode profiles of the first three cladding modes for the step waveguide, (a), and the 0.009-triangular waveguide, (b). In the step waveguide, the cladding modes exhibit an oscillatory behavior in the entire radial direction and the intensity near the core increases for higher order modes, as shown in Fig. 5 (a). In the case of the triangular index profile, however, the field is much more confined to the core region for the lower order modes, which contributes to the larger overlap integral in Eq. (5). These confined cladding modes may introduce modal interference with the core mode in the standard single mode fiber. However it is easy to strip off the residual cladding modes with an evanescent wave filter proposed by the authors. [18]

IV. LONG PERIOD GRATING SPECTRAL ANALYSIS

From Eq. (1), the phase matching grating pitch, Λ, was calculated as a function of the coupling wavelength and results are shown in Fig. 6 for the first 9 cladding modes. The results for the step index profile are shown in Fig. 6 (a), those for the 0.009-triangular index profile in Fig. 6 (b), and those for the trapezoidal (Trap-2) index profile in Fig. 6 (c), respectively. Compared with the results of the step waveguide, the phase matching conditions for the triangular and trapezoidal index profiles show significant differences in terms of the slope in the plot of the grating pitch versus the resonance wavelength. The slope is shallower in the triangular and trapezoidal waveguide compared with the step waveguide, which is attributed to the modification of dispersion of cladding modes as indicated in Fig. 3. Another notable feature is that the spacing between the spectral resonances is significantly wider in the proposed waveguides than that in step waveguide, which directly indicates a wider free spectral range. The results in Fig. 3 are consistent with the observations in Fig. 6.

From the phase matching condition, Eq. (1), the resonance wavelength of m-th order and $(m+1)$-th

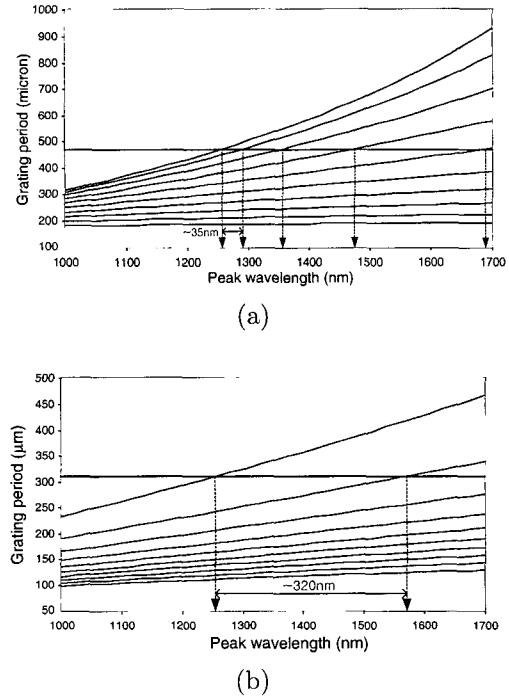

FIG. 6. Plot of the phase matching grating pitch, Λ, versus the coupling wavelength for the first 9 cladding modes. The results for the step waveguide are shown Fig. (a), those for the 0.009 triangular waveguide in Fig. (b), and those for the trapezoidal (Trap-2) waveguide in Fig. (c).

order cladding modes can be expressed as ;

$$\lambda_m = \Lambda\left[n_{11}^{eff}(\lambda_m) - \left\{n_{1m}^{eff}(\lambda_m) + \Delta n_{1m}^{eff}(\lambda_m)\right\}\right], \tag{7}$$

$$\lambda_{m+1} = \Lambda\left[n_{11}^{eff}(\lambda_{m+1}) - \left\{n_{1m+1}^{eff}(\lambda_{m+1}) + \Delta n_{1m+1}^{eff}(\lambda_{m+1})\right\}\right], \tag{8}$$

here n_{11}^{eff} is the effective index of the fundamental core mode(HE_{11}), n_{1m}^{eff} and n_{1m+1}^{eff} are the effective indices of m-th order (HE_{1m}), and $(m+1)$-th order (HE_{1m+1}) cladding modes in step index cladding fiber, and Δn_{0m}^{eff} and Δn_{0m+1}^{eff} are the effective indices change of m-th order and $(m+1)$-th order cladding modes due to refractive index change in the cladding. Using Eqs. (7) and (8), the wavelength separation between m-th and $(m+1)$-th cladding mode, $\delta\lambda_{m,m+1}$, or equivalently the free spectral range of a LPG can be expressed as;

$$\delta\lambda_{m,m+1} = \Lambda\left[\left\{n_{11}^{eff}(\lambda_{m+1}) - n_{11}^{eff}(\lambda_m)\right\} - \left\{n_{1m+1}^{eff}(\lambda_{m+1}) - n_{1m}^{eff}(\lambda_m)\right\} + \left\{\Delta n_{1m}^{eff}(\lambda_m) - \Delta n_{1m+1}^{eff}(\lambda_{m+1})\right\}\right]. \tag{9}$$

In order to solve this transcendental equation for the resonance wavelengths, λ_m and λ_{m+1}, effective indices of the first two cladding modes were numerically obtained as shown in Fig. 7. In this figure, we focused on the 1st cladding mode where the coupling was set to take place at 1300 nm along with its nearest neighboring 2nd mode for the step and triangular cladding index profiles. Note that in Fig. 7, both the slopes and the magnitude of the effective indices did change as a function of degree of the refractive index suppression or the index differences given from 0.003 to 0.009. Keeping the resonance of 1st mode at 1300 nm by adjusting grating pitches, the transcendental Eq. (9) was numerically solved to obtain the free spectral range, $\lambda_2 - \lambda_1$ as a function of the index difference in the triangular profile. The grating pitch for the step index cladding, , was set to 470 μm. As the cladding index further suppressed from 0.003, 0.006, to 0.009 in the cladding, the grating pitches were varied from 369, 329 and 316 μm, respectively. See Fig. 6 for phase matching conditions. The numerical results on free spectral ranges are shown in Fig. 8. As the refractive index difference in the triangular profile, the free spectral range monotonically increases from 37 nm to 322 nm, by a factor of ~9.

Transmission spectra of LPGs were numerically

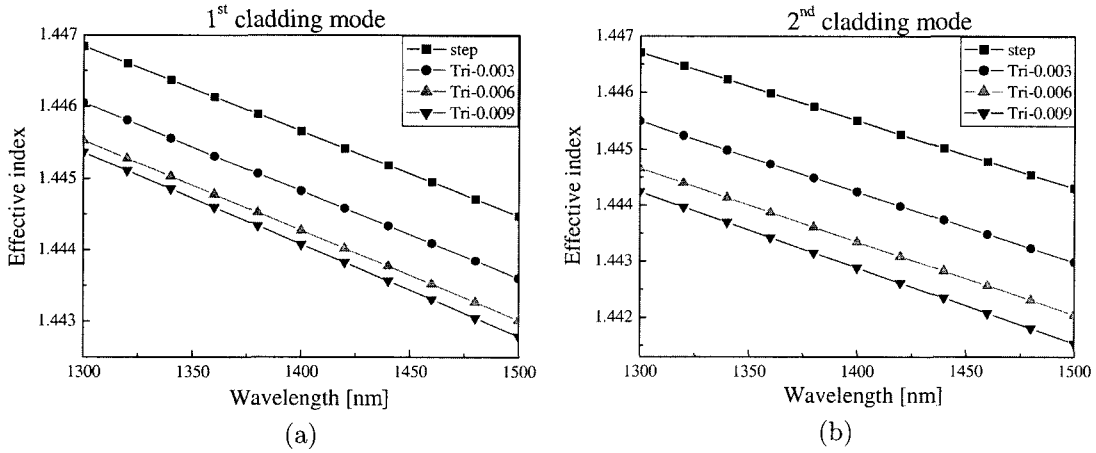

FIG. 7. Effective indices of 1st, (a), and 2nd, (b), cladding modes for step and triangular waveguides. Both material dispersion, calculated from Eq. (2), and waveguide dispersion are included in calculations. Absolute effective index slopes of 1st and 2nd cladding modes increased as much as by ~0.1082×10^{-5} (~8.7 %) and ~0.1457×10^{-5} (~11.4 %) reference to conventional step waveguide for the 0.009 triangular waveguide.

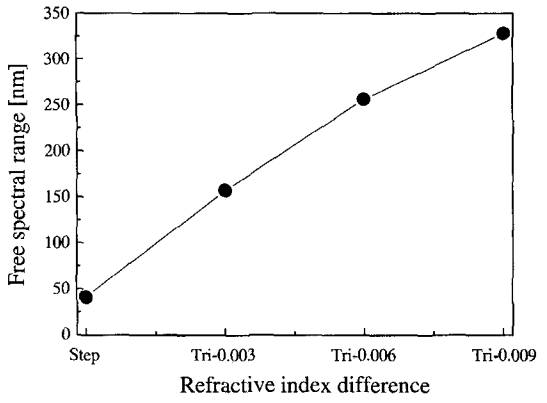

FIG. 8. Free spectral range as a function of refractive index difference in the triangular waveguides.

simulated using the overlap integral equations, (5)−(6), for various cladding index profiles. Induced index change, $\Delta n_{induced}$, was assumed to be uniform over the cross section of the fiber core. A uniform step function was assumed for the periodic index grating structure along the core of the fibers in order to simplify numerical analysis. In the grating structure radial and angular dependence were not considered. Neither chirping nor apodization were assumed to focus on the waveguide dispersion of cladding modes. A periodic index modulation of a step function with the amplitude of $\Delta n_{induced}$, with the duty cycle of C, was assumed along the length of L in the core and numerical values for these parameters are; $\Delta n_{induced}$ =0.0003−0.0005, C=0.5, and L=25.4 mm, similar to those previously reported in reference. [15] The grating pitch was adjusted as described in the previous paragraph for different refractive index profile to keep the resonance at 1300 nm. The results of numerical simulation on the LPG transmission spectra are shown in Fig. 9. By inducing triangular profile into the clad region, and consequently changing the waveguide dispersion of cladding modes, we could isolate only one

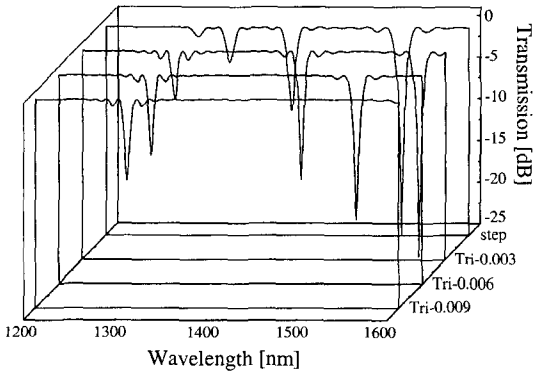

FIG. 9. Long period grating transmission spectra for various cladding index profiles.

cladding mode resonance peak of LPG in the spectral range from 1200 nm to 1600 nm at the 0.009-triangular waveguide. The free spectral range was estimated about 330 nm as shown in Fig. 8. We, therefore, confirmed that the proposed technique to modify the cladding index profile does control the free spectral range. Selective flattening of a gain band without incurring insertion loss in the neighboring bands can be achieved using LPGs utilizing the proposed fiber structures. For the trapezoidal profile, we couldn't achieve isolation of only one cladding mode resonance peak, but the free spectral range was increased to about 200 nm. Novel filtering devices could be further designed whose characteristics will be confined only to the wavelength region of interests with negligible cross talk among adjacent bands.

V. CONCLUSION

A new optical fiber structure that modifies the cladding mode waveguide dispersion was proposed for fiber filters based on coupling between the core and cladding-modes. The effects of modification of the refractive index profile in the cladding region on the waveguide dispersion of cladding modes were theoretically analyzed using finite-difference analysis and coupled mode theory. Effective index decrease of over 1.7×10^{-3}, or by a factor of ~0.12 % referenced to a step waveguide was theoretically estimated for a triangular waveguide. This change in waveguide dispersion of the cladding mode induced significant modification in the phase matching conditions. By coupling to 1st symmetric cladding modes, enhancement of free spectral range over 300 nm was theoretically predicted, which could be applied for noble fiber filters in ultra-wide band optical communication systems.

ACKNOWLEDGEMENTS

This research is partly funded by the KOSEF through UFON ERC program in KJIST, BK21 program supported by MOE and CHOAN ITRC program supported by MIC.

*Corresponding author : koh@kjist.ac.kr.

† H. Jeong was with KJIST and is now with the Micro Mechatronics team, Korea Institute of Industrial Technology, ChonAn-si, KOREA.

REFERENCES

[1] A. M. Vengsarkar, P. J. Lemaire, J. B. Judkins, V. Bhatia, and T. Erdogan, "Long-period fiber gratings as band-rejection filters," *J. Lightwave Technol.*, vol. 14, pp. 58–65, 1996.

[2] A. S. Kurkov, M. Douay, O.Duhem, B. Leleu, J. F. Henninot, J. F. Bayon, and L. Rivoallan, "Long-period fiber grating as a wavelength selective polarization element," *Electron. Lett.*, vol. 33, pp. 616–617, 1997.

[3] H. J. Patrick, G. M. Williams, A. D. Kersey, J. R. Pedrazzani, and A. M. Vengsarkar, "Hybrid fiber Bragg grating/long period fiber grating sensor for strain/temperature discrimination," *IEEE Photonics Technol. Lett.*, vol. 8, pp. 1223–1225, 1996.

[4] T. Komukai, T. Yamamoto, T. Sugawa, and Y. Miyajima, "Upconversion pumped thulium-doped fluoride fiber amplifier and laser operation 1.47 μm," *IEEE Quantum Electron.*, vol. 31, pp. 1880–1889, 1995.

[5] J. Kani, M. Jinno, and K. Oguchi, "Fiber Raman amplifier for 1520-nm band WDM transmission," *Electron. Lett.*, vol. 34, pp. 1745–1747, 1998.

[6] R. I. Laming, M. N. Zervas, and D. N. Payne, "Erbium-doped fiber amplifier with 54 dB gain and 3.1 dB noise figure," *IEEE Photon. Technol. Lett.*, vol. 4, pp. 1345–1347, 1992.

[7] J. F. Massicott, R. Wyatt, and B. J. Ainslie, "Low noise operation of Er3+-doped silica fibre amplifier around 1.6 μm," *Electron. Lett.*, vol. 28, pp. 1924–1925, 1992.

[8] S. A. Vasiliev, E. M. Dianov, D. Varelas, H. G. Limberger, and R. P. Salathe, "Postfabrication resonance peak positioning of long-period cladding-mode-coupled gratings," *Opt. Lett.*, vol. 21, pp. 1830–1832, 1996.

[9] Qun Li, Xiaoming Liu, Jiangde Peng, Bingkun Zhou, E. R. Lyons, and H. P. Lee, "Highly efficient acoustooptic tunable filter based on cladding etched single-mode fiber," *IEEE Photon. Technol. Lett.*, vol. 14, pp. 337–339, 2002.

[10] J. R. Clowes, J. McInnes, M. N. Zervas, and D. N. Payne, "Effects of high temperature and pressure on silica optical fiber sensors," *IEEE Photon. Technol. Lett.*, vol. 10, pp. 403–405, 1998.

[11] H. Jeong and K. Oh, "Enhancement of free spectral range of the resonance peaks in a long-period fiber grating by controlling material dispersion of cladding modes," *Opt. Commun.*, vol. 199, pp. 103–110, 2001.

[12] J. W. Fleming, "Material dispersion in lightguide glasses," *Electron. Lett.*, vol. 14, p. 326, 1978.

[13] J. Kirchhof, S. Unger, and K.-F. Klein, "Diffusion behavior of fluorine in fiber lightguide materials," *Optical Fiber Communication Conference (OFC/IOOC) '93*, technical digest, paper WG4, 1993.

[14] M. Stern, *Finite-difference analysis of planar optical waveguides*, Chapter 4, in PIER 10 (Progress in Electromagnetic Research 10) edited by W. P. Huang, Cambridge, Massachusetts, EMW Publishing, 1995.

[15] T. Erdogan, "Cladding-mode resonances in short- and long-period fiber grating fibers," *J. Opt. Soc. Am. A*, vol. 14, pp. 1760–1773, 1997.

[16] C. Tsao, *Optical fibre waveguide analysis*, Chapter 10, Oxford, New York, Oxford University Press, 1992.

[17] J. W. Fleming and D. L. Wood, "Refractive index dispersion and related properties in fluorine doped silica," *Applied Optics*, vol. 22, pp. 3102–3104, 1983.

[18] K. Oh, U. C. Ryu, S. Kim, J. Yu, H. Jeong, and U. C. Paek, "Evanescent wave filter made of optical fiber with Er doped ring in the inner cladding," *Optoelectronics and communications conference'2000*, Tech. Dig. paper 12P-49, Chiba, Japan, 2000.